JOURNAL OF MATERIALS SCIENCE: MATERIALS IN MEDICINE **16** (2005) 161 – 165

Fabrication of hydroxyapatite ceramics with controlled pore characteristics by slip casting

XIUMIN YAO*, SHOUHONG TAN, DONGLIANG JIANG
The State Key Laboratory of High Performance Ceramics and Superfine Microstructure, Shanghai Institute of Ceramics, Chinese Academy of Sciences, Shanghai 200050
E-mail: yaoxmin@yahoo.com

Porous hydroxyapatite (HAp) ceramics with controlled pore characteristics were fabricated using slip casting method by mixing PMMA with HAp powder. The optimum conditions of HAp slip for slip casting was achieved by employing various experimental techniques, zeta potential and sedimentation, as a function of pH of the slips in the pH range of 4–12. HAp suspensions displayed an absolute maximum in zeta potential values and a minimum in sedimentation height at pH 11.5. The optimal amount of dispersant for the HAp suspensions was found at 1.0 wt% according to the viscosity of 25 vol% HAp slurry. The rheological behaviour of HAp slurry displays a shear-thinning behavior without thixotropy, which is needed in slip casting processing. The pore characteristics of sintered porous hydroxyapatite bioceramics can be controlled by added PMMA particle size and volume. The obtained ceramics exhibit higher strength than those obtained by dry pressing.

1. Introduction

Hydroxyapatite (HAp) and related calcium phosphate (CP) materials have been widely used as implant materials for many years due to their close similarity in composition and high biocompatibility with nature bone [1–4]. Recently, a number of reports have emphasized the fabrication and properties of porous HAp Ceramics [5–9]. The bone can grow in the pore, however, as indicated by Hulbert *et al*. [10], macropores of at least 100 μm are needed to host the cellular and extracellular components of bone and blood vassels, and greater than 200 μm are expected to be effective on osteoconduction. Therefore, how to control the pore characteristics in the porous HAp ceramic is an important subject for many investigations. Although the pore size or pore size distribution is directly related to the particle size distribution of introduced polymeric powders, it is rather difficult to obtain porous HAp ceramic with complex geometry via conventional die-pressing route [7, 11–13]. Then, some researchers have demonstrated several methods to produce porous hydroxyapatite ceramics [5, 8, 13–18].

In this study, porous HAp ceramics with controlled porosity were prepared by slip casting method with polymethyl methacrylate (PMMA) particles used as a porosifier. The influence factors of HAp slurry properties are discussed. The influences of PMMA particle size and volume fractions on the resultant pore characteristics of porous HAp ceramics were also investigated.

2. Experimental procedure

2.1. Materials

Hydroxyapatite (HAp) powder (Ca/P = 1.69, D = 3.16 g/cm^3, Sichuan University, China) was used as raw material in this study. Spherical polymethyl methacrylate (PMMA) (Coral Chemistry Factory of Shanghai, China) with different particle sizes, 260–350 μm, 120–150 μm, and 50–75 μm, was used as porosifier, the average particle sizes of it are 305 μm, 134 μm, 62 μm, respectively. Polyacrylic acid (PAA) (30 wt%, Nanjing College of Chemical Engineering, China) with molecular weight less than 15,000 was used as dispersant. Polyvinyl alcohol (PVA) (Jinshan Petrochemical Works, China) with a 280,000 molecular weight was used as binder.

2.2. Experimental procedure

HAp powders with dispersant were milled in a ball jar at pH 11.5 for 12 h, using zirconia balls as grinding media. The pH value of the slurry was adjusted by 1 N NaOH or 1 N HCl. Then, PMMA particles and PVB (2.0 wt%, relative to the solids) were added into the ball jar. After another 12 h, the slurries, free of foam, were cast into plaster molds. After demolded and dried at ambient temperature for 72 h, the green blocks were heated to 550 °C at a heating rate of 0.5 °C/min to burn out the PMMA particles and other volatiles, followed by the treatment at 1200 °C for 2 h for densification purpose.

*Author to whom all correspondence should be addressed.

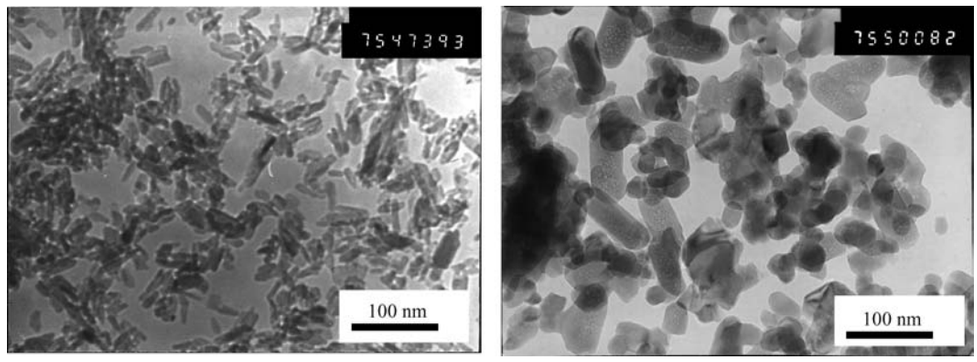

(a) (b)

Figure 1 TEM morphology of HAp powders: (a) Initial HAp powder and (b) Calcined HAp powder (800 °C × 2 h).

2.3. Characterization

The specific area of HAp powders was measured by accelerated surface area and porosimetery system (ASAP 2001, Micromeritics, America). The X-ray diffraction patterns of powders were tested by X-ray instrument (X-ray diffractometer, Model RAX-10, Rigaku, Japan). The Zeta-potential of powders at various pH values was measured by electrophretic mobility instrument (JSD-94). The viscosity and thixotropy were studied by coaxial flat rheometry (SR-5 Rheometric scientific instrument company, America). The sedimentation behavior of the HAp slips was studied as a function of time at different pH values (2–12) for 5 vol% solids loading. The sedimentation heights were measured from the bottom of the sediment test tube to the height of the solid deposited after specific intervals of time.

The relative density and porosity were measured by Archimedes methods. The open porosity

$$p_o = \frac{m_2 - m_1}{m_2 - m_3} \times 100\%,$$

the close porosity

$$p_c = \frac{(m_1 - m_3) - m_1 \times \rho_t}{m_2 - m_3} \times 100\%,$$

the total porosity $P_t = P_o + P_c$. Where, m_1 is the dry weight of the simples measured in air, m_2 is the weight of the sample measured under water soaked in air, m_3 is the weight of the simple measured under water soaked in water, ρ_t is the theoretical density of HAp.

The macropores size distributions were analyzed by LeicaQwin software of image analysis (Leica coporation, GDR). The microstructure of the composites was observed on a fractured surface by scanning electron microscopy (SEM) (model EPMA-8705Q, HII, Shimadzu, Japan). The flexural strength of porous HAp ceramics was measured in Instron 1195 universal testing machine by three-point flexure, using a span of 30 mm and a crosshead speed 0.5 mm/min.

3. Results and discussion

3.1. Surface properties of HAp powders

Fig. 1 shows the morphology of HAp powders. The average radial particle size of initial powder was less than 50 nm. In order to get higher solid contents, the initial HAp powder, which was too fine to get high solid content, was calcined at 800 °C for 2 h. After calcination, The contrastive morphology and X-ray patterns of HAp powder were respectively showed in Figs. 1 and 2. TEM photographs of HAp powders shows calcined HAp powders have bigger particle sizes, which was also testified by the specific area of HAp powders (after calcinations, the specific area decreased from 73.08 m^2/g to 25.51 m^2/g). Fig. 2 shows that no phase transformations were detected. and calcined HAp powder has a sharper peaks than initial. According to Scherrer formular [19], sharper peaks means bigger crystalline size.

Zeta-potentials of nanosized HAp powder at different pH value, dispersed in water containing 1.0 wt% PAA (relative to the solids) or without PAA, were measured. As shown in Fig. 3, after adding the dispersant, the pH value at the isoelectric point of HAp powders decreased from approximately pH 6.2 to pH 4.7. The addition of PAA decreased the zeta potential of the powders, which is beneficial to dispersion of HAp particles by electrostatic repulsion. Also the both zeta potential curves showed an absolute maximum value at pH 11.5, indicating that the slurries could be well dispersed at the pH value.

3.2. Sedimentation behavior

The sedimentation volume percent as a function of pH is shown in Fig. 4. At pH < 7, added PAA was adsorbed

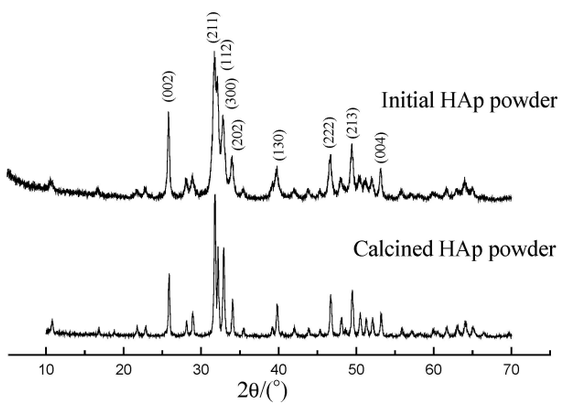

Figure 2 XRD of HAp powders.

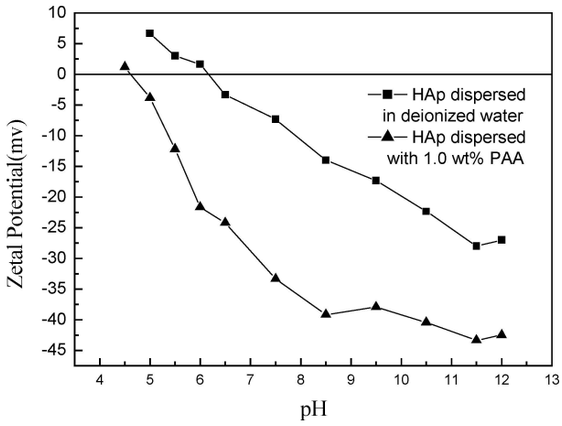

Figure 3 Zeta-potential as a function of pH for HAp powder.

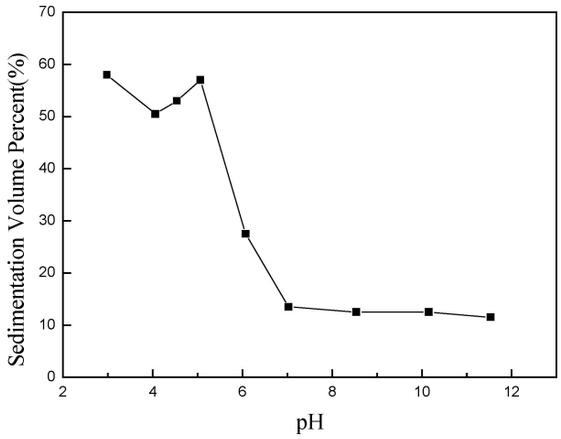

Figure 4 Sedimentation volume as a function of pH for 5 vol% HAp suspension after 7 days.

on the surface of HAp powders as neutral PAA [20, 21] and the repulsive energy between HAp powders was low. Therefore, HAp powders were easily agglomerated, which was confirmed by the high sedimentation volume and the clear supernatant liquid.

At pH > 7, some PAA reacted with NaOH solution which was added for pH adjustment to form polyacrylic sodium (PAANa) and be adsorbed as ionic PAANa [20, 21]. The adsorbed ionic PAANa increased the electrostatic repulsive energy between HAp particles, which improved the dispersion property of HAp in this zone. The sedimentation volume decreased apparently and had no significant variation up to pH 12. HAp powders can be well dispersed at pH > 7. The Zeta-potential value reached the absolute maximum value at pH 11.5. Therefore, pH 11.5 was chosen as optimal dispersion pH value.

3.3. Slurry rheological behavior

3.3.1. Effect of dispersant content

Viscosity of 25 vol% HAp suspensions with different PAA contents (relative to the solids) has been measured at pH 11.5 (Fig. 5). At PAA content <0.6, viscosity of slurry decreases with increasing PAA content. In the aqueous medium, the dissociated PAA may cover the

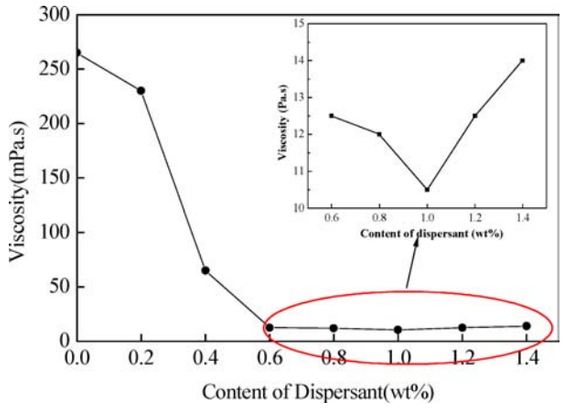

Figure 5 Viscosity of 25 vol% HA slips as a function of dispersant contents at pH 11.5.

surface of HAp powders and the HAp powders would behave as a monodispersed powder due to the electrosteric stabilization, resulting in a decrease in viscosity of the slurry. At 0.6–1.0 wt% PAA, the viscosity changes a little and the minimum viscosity value is observed at 1.0 wt% PAA content. This may indicate the adsorbed PAA on the surface of the HAp powders is enough to prevent HAp particle-particle attraction. When the added PAA content is higher than the saturated PAA absorption point, the free PAA would exist in the liquid medium. This may cause inter-locking of PAA polymer chain, which bridged the solid particles and caused viscosity increase. Therefore, 1.0 wt% PAA was chosen as optimum dispersant amount.

3.3.2. Effect of solids loading

The effect of solid loading on the flow behavior of HAp slurry in distilled water at pH = 11.5 is shown in Fig. 6. Shear thinning behavior [22] was observed at solid loading of 20–35 vol%. And with the increase of the solids loading, the viscosity increased. But at the same solid loading, the viscosity decreased as shear rates increased. The shear-thinning behavior with the shear rate increasing shows that viscosity is strongly dependent on the solid loading. But when solid loading

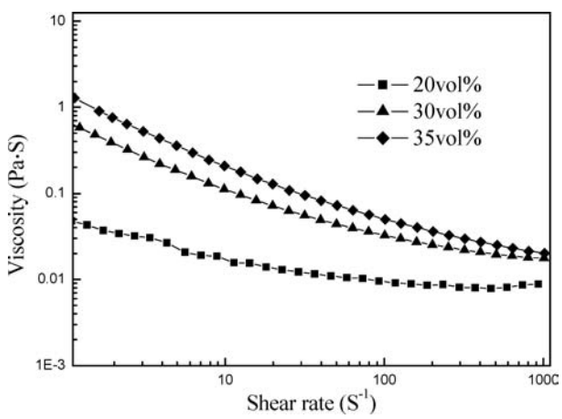

Figure 6 Rheological curves for the slurries prepared at different HAp solid loadings.

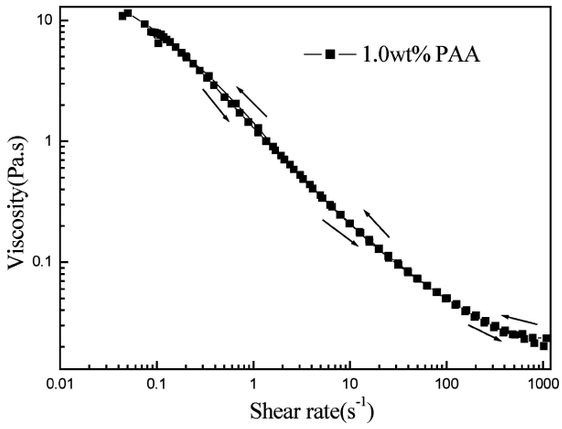

Figure 7 Rheological curve of 35 vol% HAp slurry containing 1.0 wt% PAA.

was above 40 vol%, it was difficult to get slurry with well rheological properties in the study. The rheological behavior of HAp slurry at 35 vol% solid loading has been studied by measuring the viscosity and shear stress at varying shear rates (Fig. 7). There was no thixotropy, which means that 35 vol% solid loading HAp slip is suitable to slip casting.

3.4. Microstructure and properties of porous HAp ceramics

Fig. 8 shows that the pores of porous HAp ceramics are spherical with the same shape of adding PMMA particles (Fig. 9) and uniformly distributed, which indicates that the shape of pores didn't change during sintering process. However, as the average particle size of added PMMA are 305 μm, 134 μm, 62 μm, the average pore size of porous HAp ceramics are 290 μm, 96 μm, 45 μm, respectively. That is to say, as shown in Fig. 8 (a)–(c), the mean diameter of the pores is smaller than the particle size of added PMMA, which may be caused by the shrink of the ceramics during sintering process. A detailed examination of the solid walls (Fig. 8(d)) revealed the presence of micropores in the scale of $\sim$1 μm, which was considered to be the result of sintering effect.

As shown in Table I, the total porosity of the porous HAp ceramics is little influenced by variation of the PMMA particle size at a given volume fraction of PMMA, under the same sintering conditions. And the total porosity of the porous HAp ceramics is roughly equal to the initial PMMA volume fraction. Therefore, the porosity of porous HAp ceramics can be modulated as the added PMMA volume changed.

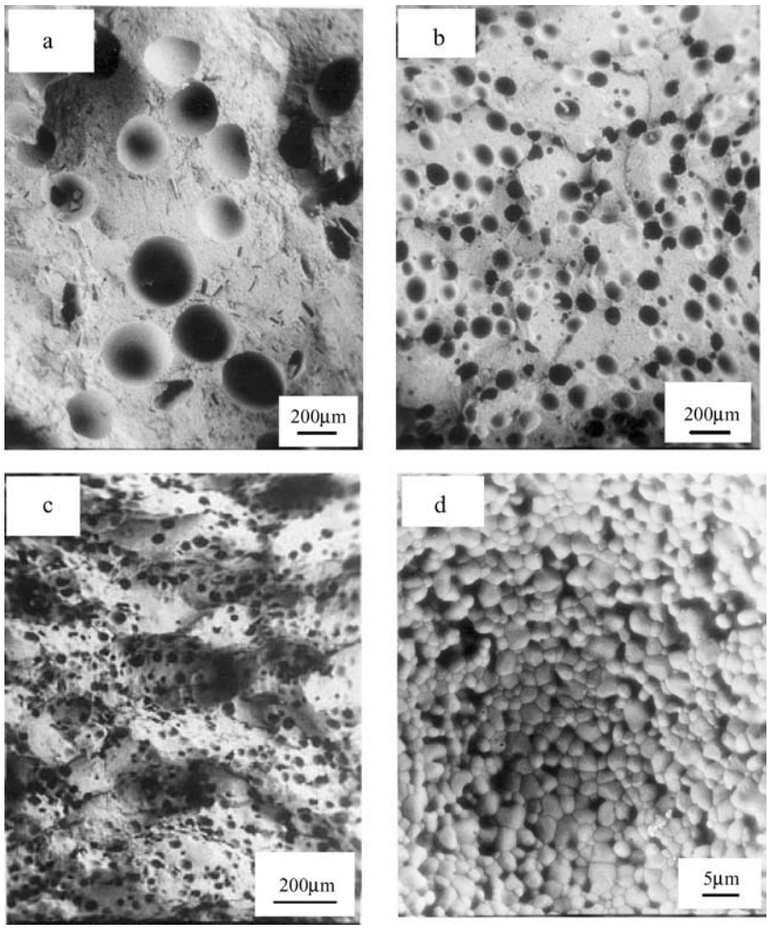

Figure 8 SEM photographs of porous HAp ceramics prepared by slip casting. (a) PMMA 30 vol% size between 260–350 μm, (b) PMMA 36 vol% size between 120–150 μm, (c) PMMA 36 vol% size between 50–75 μm, and (d) Micropore of porous HA ceramics.

TABLE I Properties of porous HAp ceramics by slip casting as a function of PMMA

Volume fraction/vol%	Particle sizes/μm	Bending strength/MPa	Open porosity/%	Closed porosity/%	Total porosity/%
36	120–150	15.74 ± 1.74	39.04	0.64	39.68 ± 0.62
	260–350	12.53 ± 1.16	33.00	0.48	33.48 ± 0.20
30	120–150	18.38 ± 1.36	32.22	0.70	32.92 ± 0.45
	50–75	26.12 ± 1.21	29.04	0.51	29.55 ± 0.71
23	120–150	21.33 ± 1.94	23.82	1.56	25.38 ± 0.35

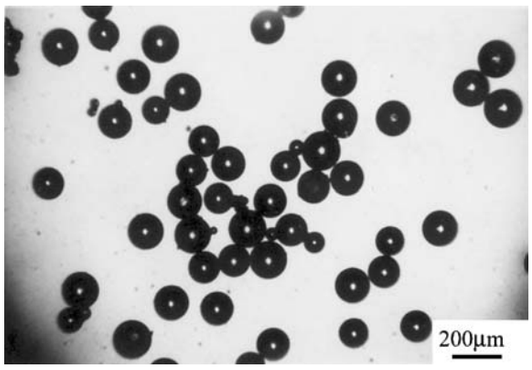

Figure 9 Optical photo of PMMA particles (particle sizes between 120–150 μm).

The mechanical properties of the porous ceramics in terms of the porosity and pore sizes are shown in Table I. The influence of pore sizes on the flexural strength has currently found to be important in producing the porous HAp ceramics. The larger the pore size, the lower the flexural strength is at the same given volume fraction of the PMMA. At the same PMMA particle size, the strength decreases as the volume fraction increases. When added PMMA particle size is 120–150 μm, the bending strength of porous HAp with 30 vol% PMMA made by slip casting is, about as five times as that of ceramics made by dry pressing (18.38 MPa and 3.97 MPa, respectively). Therefore, slip cast processing proves to be a suitable technique to prepare porous HAp ceramics with controlled pore characteristics.

4. Conclusions

The fabricating process and properties of the porous HAp ceramic by slip casting were studied. By studying the zetal potential and sedimentation behavior of HAp slips in the pH range 4–12, the pH value of best dispersion was chosen at pH 11.5. The optimum dispersant amount, 1.0 wt%, was decided by analysis of the viscosity of 25 vol% HAp slip. 35 vol% HAp slurry showed shear thinning behavior nearly without thixotropy, which is suitable for slip casting to produce porous HAp ceramics. The pore characteristics of sintered porous hydroxyapatite bioceramics can be controlled by changing the size and content of PMMA. Also the ceramics had higher strength than those made by dry pressing.

References

1. L. L. HENCH, *Ceram. Inter.* **22** (1996) 493.
2. G. DACULSI, *Biomaterials* **19** (1998) 1473.
3. S. YAMADA, D. HEYMANN, J. M. BOULER and G. DACULSI, *J. Biomed. Mater. Res.* **37** (1997) 348.
4. K. DE. GROOT, *Biomaterials* **1** (1980) 47.
5. E. RIVERA-MUNOZ, J. R. DIAZ and J. R. RODRIGUEZ, *J. Mater. Sci: Mater in Med.* **12** (2001) 305.
6. L. L. HENCH, *J. Am. Ceram. Soc.* **81** (1998) 1705.
7. D. M. LIU, *Key Engineering Materials* **115** (1996) 209.
8. D.-M. LIU, *Ceram. Inter.* **24** (1998) 441.
9. LIU DEAN-MO, *J. Mater. Sci. Letter.* **15** (1996) 419.
10. S. F. HULBERT, S. J. MORRISON and J. J. KLAWITTER, *J. Biomed. Mater. Res.* **2** (1970) 269.
11. J. C. LE HUEC, *Biomaterials* **16** (1995) 113.
12. R. W. RICE, *J. Mater. Sci.* **28** (1993) 2187.
13. XIUMIN YAO, SHOUHONG TAN and DONGLIANG JIANG, *Inorganic Materials (in Chinese)* **15** (2000) 467.
14. I. H. ARITA, D. S. WILKINSON, M. A. MONDRAGÓN and V. M. CASTAÑO, *Biomaterials* **5** (1995) 403.
15. S. TAKAGI and L. C. CHOW, *J. Mater. Sci: Mater in Med.* **1** (1995) 19.
16. D. M. LIU, *Ceram. Inter.* **2** (1997) 135.
17. O. GAUTHIER, J. M. BOULER, *et al.*, *Biomaterials* **1–3** (1998) 133.
18. E. RIVERA-MUNOZ, J. R. DIAZ, J. ROGELIO RODRIGUEZ, W. BROSTOW and V. M. CASTANO, *J. Mater. Sci: Mater in Med.* **4** (2001) 305.
19. H. P. KLUG and L. E. ALEXANDER, "X-ray Diffraction Procedures for Polycrystalline and Amorphous Materials" (Wiley, New York, NY, 1997) p. 637.
20. Y. HIRATA, J. KAMIKAKIMOTO, A. NISHIMOTO and Y. ISHIHARA, *J. Ceram. Soc Japan* **1** (1992) 7.
21. V. A. HACKLEY, *J. Am. Ceram. Soc.* **9** (1997) 2315.
22. R. MEREMO, *Am. Ceram. Soc. Bull.* **71** (1992) 1521 (Elsevier Science Publishing Company Inc, Netherlands, 1989) p. 16.

Received 20 October 2003
and accepted 30 June 2004